A&A 528, A125 (2011)
DOI: 10.1051/0004-6361/200912671
© ESO 2011

Astronomy & Astrophysics

Star formation in the "Gulf of Mexico"

T. Armond[1,⋆], B. Reipurth[2], J. Bally[3], and C. Aspin[2,⋆⋆]

[1] SOAR Telescope, Casilla 603, La Serena, Chile
e-mail: tarmond@ctio.noao.edu
[2] Institute for Astronomy, University of Hawaii at Manoa, 640 N. Aohoku Place, Hilo, HI 96720, USA
e-mail: [reipurth;caa]@ifa.hawaii.edu
[3] Center for Astrophysics and Space Astronomy, University of Colorado, Boulder, CO 80309, USA
e-mail: john.bally@colorado.edu

Received 9 June 2009 / Accepted 6 February 2011

ABSTRACT

We present an optical/infrared study of the dense molecular cloud, L935, dubbed "The Gulf of Mexico", which separates the North America and the Pelican nebulae, and we demonstrate that this area is a very active star forming region. A wide-field imaging study with interference filters has revealed 35 new Herbig-Haro objects in the Gulf of Mexico. A grism survey has identified 41 Hα emission-line stars, 30 of them new. A small cluster of partly embedded pre-main sequence stars is located around the known LkHα 185-189 group of stars, which includes the recently erupting FUor HBC 722.

Key words. Herbig-Haro objects – stars: formation

1. Introduction

The North America nebula (NGC 7000) and the adjacent Pelican nebula (IC 5070), both well known for the characteristic shapes that have given rise to their names, are part of the single large HII region W80 (Morgan et al. 1955; Westerhout 1958). The central part of W80 is obscured by a large dust cloud (L935), that defines the "Atlantic Coast" and the "Gulf of Mexico" of the North America nebula (Herbig 1958). Bally & Scoville (1980) modeled W80 as an expanding molecular shell, a cloud being disrupted by early type stars born inside. For an overview of the region, see the review by Reipurth & Schneider (2008).

The distance to W80 has been the subject of some debate (Wendker 1968; Neckel et al. 1980; Armandroff & Herbst 1981), ranging from values of 500 pc to 1 kpc. We here adopt the commonly accepted distance of 550 ± 50 pc as estimated by Laugalys et al. (2006). This distance is consistent with the estimates of Herbig (1958), Wendker et al. (1983), Straižys et al. (1993) and Laugalys & Straižys (2002).

Many authors have made searches for the ionizing sources of W80, but until recently none were conclusive (e.g. Osterbrock 1957; Neckel et al. 1980; Bally & Scoville 1980). Comerón & Pasquali (2005) have finally found a good candidate among 2MASS detections in the cloud. They proposed that the exciting source is an O5V star (2MASS J205551.25+435224.6) located close to the geometric center of the complex. Straižys & Laugalys (2008) identified a few more possibly highly reddened O-type stars that contribute to the ionization of the North America and Pelican nebulae. Figure 1 shows all of the region and the location of the exciting sources of the complex.

In a grism survey of the W80 region, Herbig (1958) detected a population of Hα emission-line stars, LkHα 131–195, mostly T Tauri stars, including the little group LkHα 185 to 189 located within the dark lane of the Gulf of Mexico, thus demonstrating that low-mass star formation has recently taken place here.

LkHα 188 was included in the Second Catalog of Emission-Line Stars from Herbig & Rao (1972) as HRC 299. In a subsequent work, Welin (1973) detected only LkHα 185 and 189 among Hα emission-line stars in NGC 7000. Cohen & Kuhi (1979) optically identified a group of five faint stars associated with the small group containing LkHα 186 to 189, designating them as LkHα 188 G1 to G5 (although they are actually closer to LkHα 186). Infrared sources were also identified by Cohen & Kuhi near the optical group, and were designated as NGC 7000/IC 5070 IRS 3 to IRS 6, with IRS 5 showing Hα emission. All of these Hα emission-line stars were also included in the catalogs of Herbig & Bell (1988) and Kohoutek & Wehmeyer (1999). Table 1 lists the Hα emission-line stars known in the Gulf of Mexico prior to the present study.

Laugalys et al. (2006) made a photometric survey of the dark cloud L935, estimating spectral types, color indices and distances for hundreds of stars. They used a photometric method to infer Hα emission, listing 40 stars as possible Hα emitters in the total area surveyed (~1.2 square degrees). Later, the same group (Corbally et al. 2009) made a spectral analysis of the suspected young stellar objects (YSO) in the North America/Pelican region, confirming the Hα emission line in 19 stars.

In a recent study, Guieu et al. (2009) have used the *Spitzer Space Telescope* with IRAC to identify more than 1600 YSO candidates in or near the extended L935 cloud. They identify clusters and suggest that the region of the Gulf of Mexico contains the youngest stars of the complex.

In August 2010 the star LkHα 188 G4 = HBC 722 has increased in brightness by more than 4 magnitudes and appears to be a new FU Orionis star, as reported by Semkov et al. (2010), Miller et al. (2011) and Aspin et al. (in prep.).

⋆ Part of this work was performed at Centro de Astrofisica da Universidade do Porto, Rua das Estrelas, 4150-762 Porto, Portugal.

⋆⋆ Visiting Astronomer at the Infrared Telescope Facility which is operated by the University of Hawaii under contract to the National Aeronautics and Space Administration.

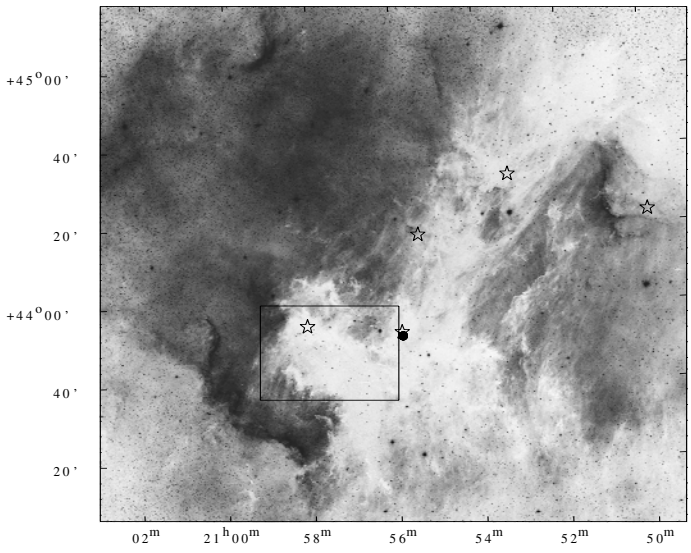

Fig. 1. The North America and Pelican nebula region, and the dark cloud that divides them, L935, in a DSS image. The black circle marks the position of the exciting source proposed by Comerón & Pasquali (2005). The asterisks mark the position of other five candidate O-type stars from Straižys & Laugalys (2008). The rectangle in the Gulf of Mexico region shows the area surveyed at Subaru telescope, corresponding to the field shown in Fig. 2. All coordinates are given in the equatorial J2000.0 system.

Table 1. Previously known Hα emission-line stars in the Gulf of Mexico.

LKHα (1)	GCVS (2)	CoKu (3)	HBC (4)	KW (5)
185	V1539Cyg		720	53-9
		NGC7000/IC5070 IRS3		53-11
		NGC7000/IC5070 IRS4		53-13
		NGC7000/IC5070 IRS5	721	53-14
		NGC7000/IC5070 IRS6		53-19
		LkHα 188 G5		53-17
		LkHα 188 G4	722	53-18
		LkHα 188 G3		53-20
		LkHα 188 G2		53-22
		LkHα 188 G1		53-23
186			723	53-24
187			724	53-25
188	V521Cyg		299	53-26
189			725	53-27

References. (1) Herbig (1958); (2) General Catalogue of Variable Stars; (3) Cohen & Kuhi (1979); (4) Herbig & Bell (1988); (5) Kohoutek & Wehmeyer (1999).

A few surveys for Herbig-Haro (HH) objects have been made in the W80 region (Ogura et al. 2002; Bally & Reipurth 2003), resulting in the identification of a number of outflows near the bright rim of the Pelican nebula. But so far no search for HH objects has been performed in the dark cloud of the Gulf of Mexico.

We present a survey for Herbig-Haro objects, for Hα emission-line stars, and for near-infrared sources in the Gulf of Mexico, and demonstrate that this molecular cloud complex is very rich in these signatures of current and recent low-mass star formation.

2. Observations

We have used a set of optical and near-infrared observations for this survey, which is summarized in Table 2.

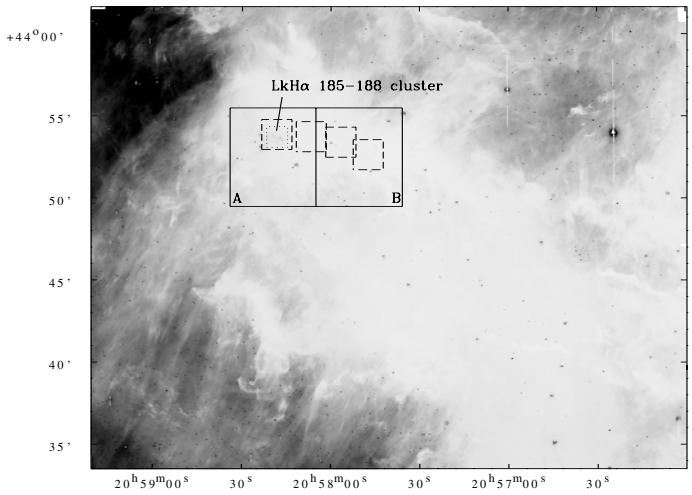

Fig. 2. Portion of the L935 dark cloud corresponding to the Gulf of Mexico, on the Hα image from the Subaru telescope taken in 2006. The two $7' \times 7'$ fields (A and B) observed at the University of Hawaii 2.2 m telescope are marked in solid lines. The full $7' \times 14'$ field corresponds to the area shown in Fig. 4. The four fields observed through an H_2 filter at UKIRT are marked with the dashed line squares. The dotted line square marks the *JHKL* field observed at IRTF, centered on the LkHα 185–188 cluster.

The University of Hawaii 2.2 m telescope on Mauna Kea was used to obtain a set of optical images of the region containing the group of stars LkHα 185 to 189. Both broad (*VRI*) and narrow band ([S II] 6717/6731 Å and Hα 6563 Å) filters were used. The Wide Field Grism Spectrograph was also used to obtain grism images with the Hα filter to detect Hα emission in the stars through slit-less spectroscopy. Previous observations obtained by George Herbig in 1998, and kindly put at our disposal, provided the opportunity to compare the emission line equivalent widths at two different epochs.

Near-infrared *JHKL* images were obtained towards the center of the optical cluster using the NASA Infrared Telescope Facility (IRTF) at Mauna Kea. The instrument used was the NSFCAM, a 1 to 5 μm imager with a 256×256 InSb detector. Reduction was carried out with standard IRAF procedures and aperture photometry was obtained with APPHOT package. The typical uncertainties for the *VRI* and *JHKL* magnitudes were of the order of 0.05 mag.

Near-infrared images were also obtained with the 4 m United Kingdom Infrared Telescope (UKIRT) at Mauna Kea, using UKIRT Fast-Track Imager (UFTI), a 1 to 2.5 μm camera with a 1024×1024 HgCdTe array. Narrow-band H_2 and [FeII] filters were used to observe selected regions. *JHK* non-photometric images were obtained to help identify embedded sources. The images were reduced with the standard UKIRT ORAC-DR pipeline.

Deep wide-field images were taken with SuprimeCam on the 8m Subaru telescope, also using Hα and [S II] filters, with seeing in individual sub-exposures ranging from 0.50″ to 0.54″ and from 0.47″ to 0.56″, respectively. The Hα image is shown in Fig. 2, where all the regions surveyed are marked.

In images from the *Spitzer Space Telescope* (Program ID #20015: IRAC and MIPS observations of the North America and Pelican nebulae, PI: Luisa Rebull), we can see the region in the mid-infrared, with many embedded sources, still invisible at near-infrared wavelengths. Those archival images were used to derive IRAC 3.6, 4.5, 5.8 and 8 μm and MIPS 24 μm magnitudes for selected stars, given in Table 6.

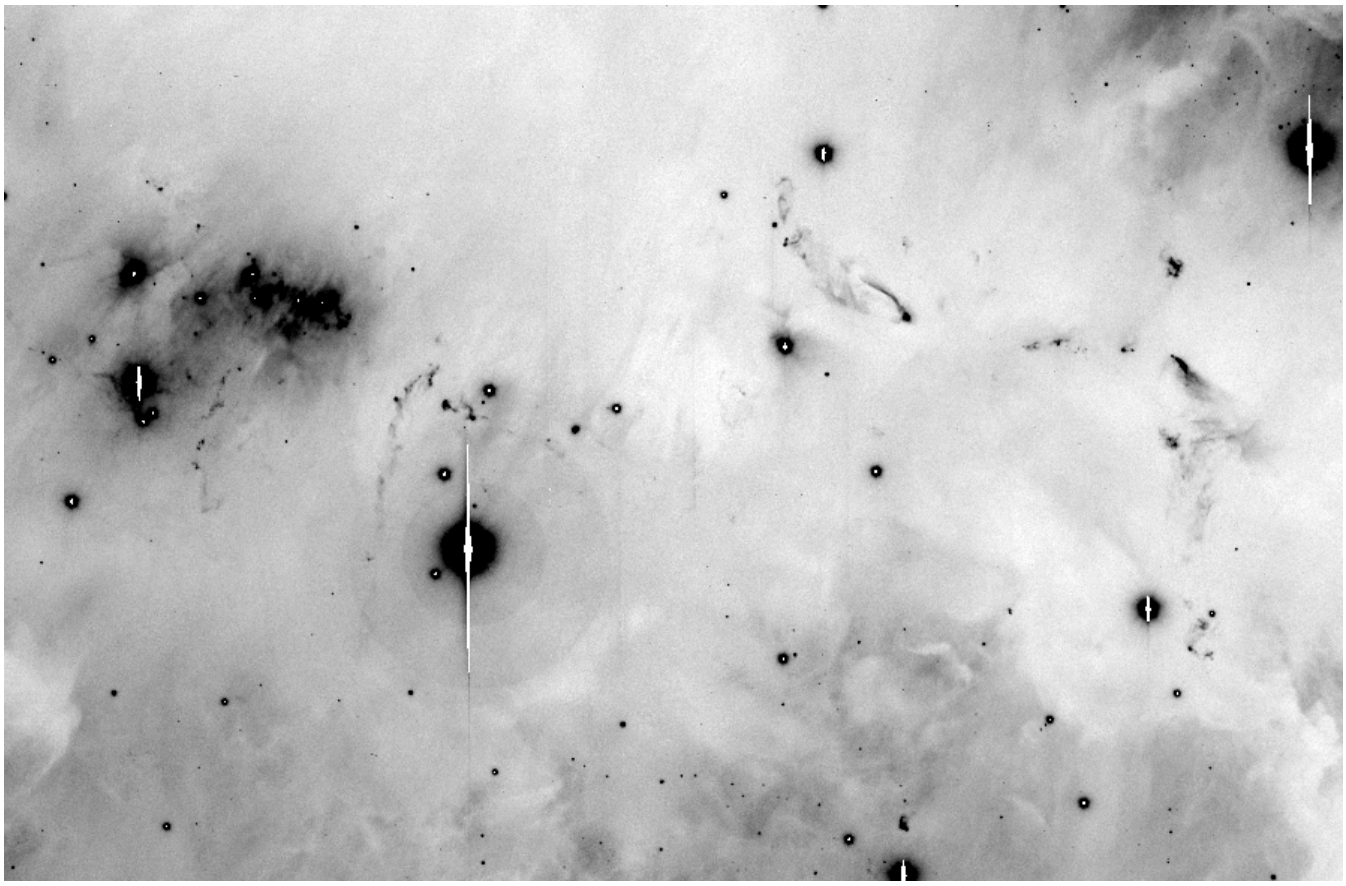

Fig. 3. A panorama of the most active region in the Gulf of Mexico based on a [S II] image from the Subaru telescope, showing most of the Herbig-Haro objects detected. The image size is approximately $6' \times 10'$. North is up and East is left.

Table 2. Observations.

Telescope/ Instrument	Date	Filters	Exp. time (s)	FOV* (′)	Plate scale (″pix^{-1})
UH 2.2 m/	2002 Jun. 16–17	*V*	1200	7 × 14 (AB)	0.22
Tek CCD		*R*	900	7 × 14 (AB)	
		I	900	7 × 7 (A)	
		[SII]	5400	7 × 7 (A)	
UH 2.2 m/	2002 Jul. 14	[SII]	5400	7 × 7 (B)	0.34
Tek CCD+WFGS		Hα	2700	7 × 14 (AB)	
		Grism	2700	7 × 14 (AB)	
	1998 Oct. 12	Grism	900	7 × 7 (A)	
UKIRT/	2002 Jul. 13	*J*, *H*, *K*	300	3 × 9	0.091
UFTI		H_2, [FeII]	500	4 × 1.5 × 1.5	
IRTF/	1999 Aug. 30	*J*	90	1.25 × 1.25	0.30
NSFCAM		*H*, *K*	30		
		L	40		
SUBARU/	2006 May 27-28	Hα	2700	34 × 27	0.20
Suprime Cam		[SII]	3000		

Notes. The fields observed are marked in Fig. 2.

3. New Herbig-Haro flows

In the [S II] and Hα images obtained with the UH 2.2 m telescope in 2002 we have found 28 HH objects. Most of them appear only in the [S II] images; the few that are detected in Hα are stronger in [S II], showing that these are low excitation shocked jet material, and not photo-ionized nebulae. Some of the flows were also detected in the near-infrared H_2 images. The broadband *I* images were also checked to prevent reflection nebulae to be identified as an HH object. The association of HH objects and H_2 knots with specific stellar sources was done by visual inspection based on proximity and apparent alignment.

In the [S II] and Hα images taken with the Subaru telescope in 2006, the amount of detail is greater and the field-of-view is much larger than in the previous images. We have detected 7 additional new HH objects on these images. One of them lies in the region surveyed in 2002, but it was too faint to be identified then.

Figure 3 shows a high contrast [S II] image from the Subaru telescope with the region containing most of the Herbig-Haro

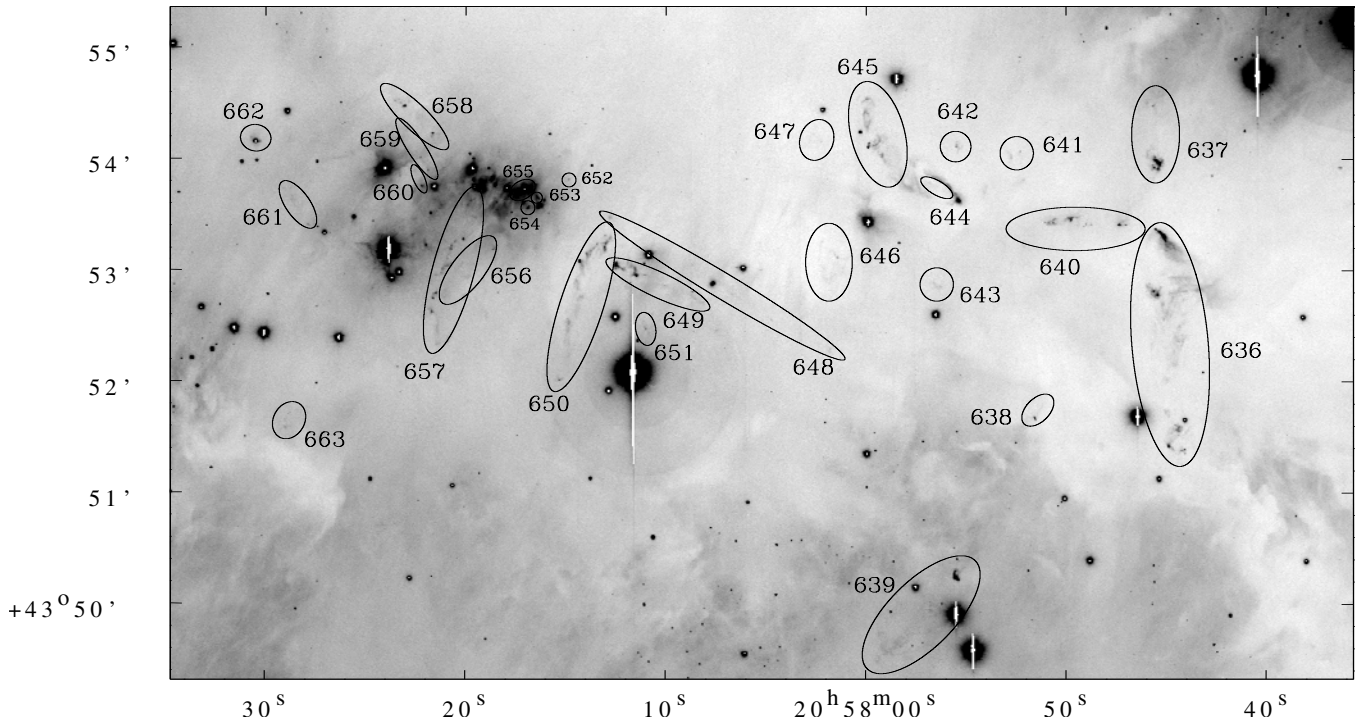

Fig. 4. Identification of new HH objects in the LkHα 185–188 cluster region. This is a [S II] image obtained at the Subaru telescope. The figure shows the area of our original survey in 2002.

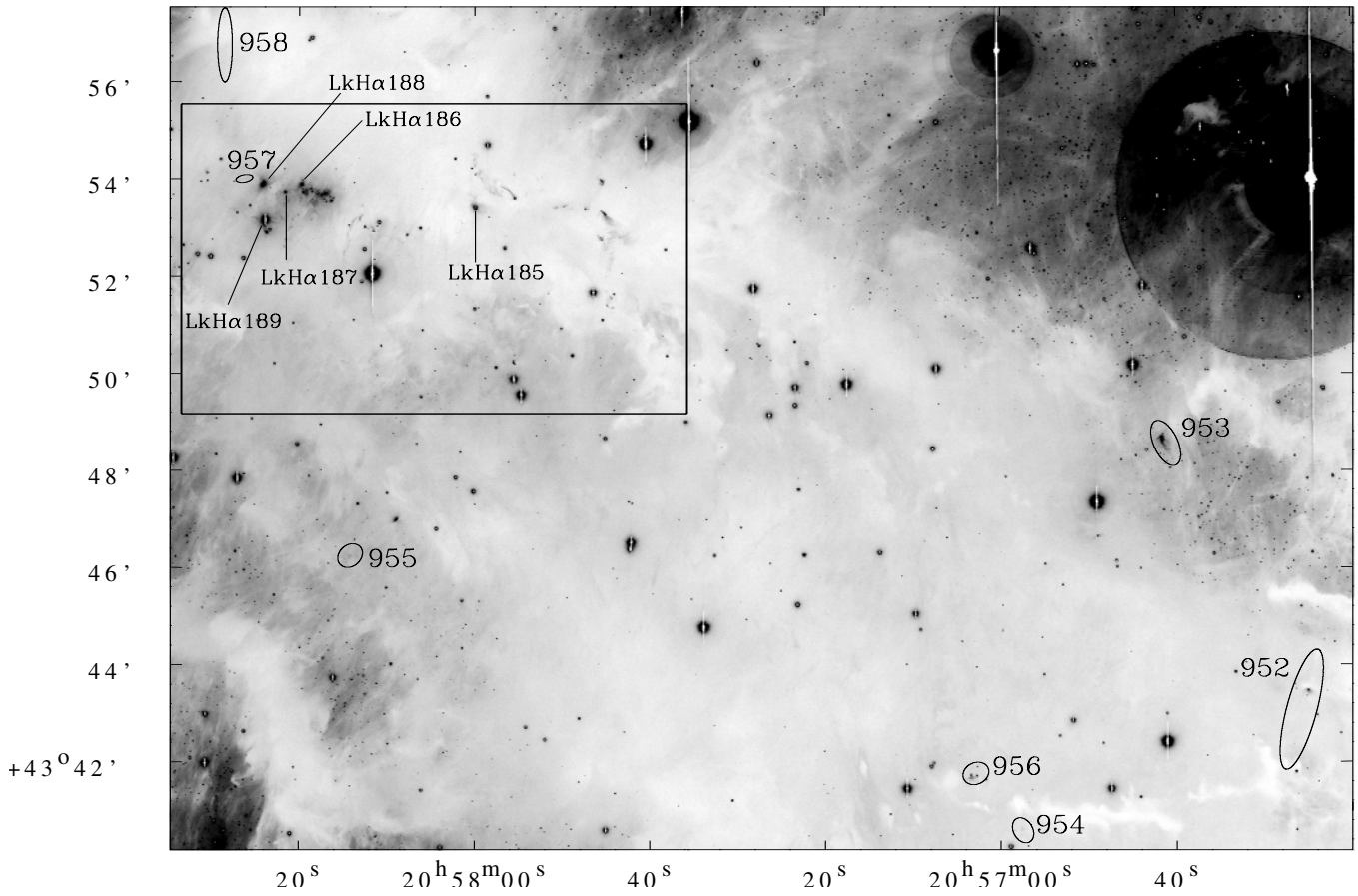

Fig. 5. [S II] image from the Subaru telescope showing the entire region surveyed for HH objects. The rectangle shows the region seen in Fig. 4. The stars LkHα 185-189 are marked.

objects found. The 35 new HH objects and their identification are shown in Figs. 4 and 5, which are also based on [S II] images. In Figs. 6 to 11 we see each set of flows in every narrow-band filter observed. Additionally, stamps of the new objects discovered in

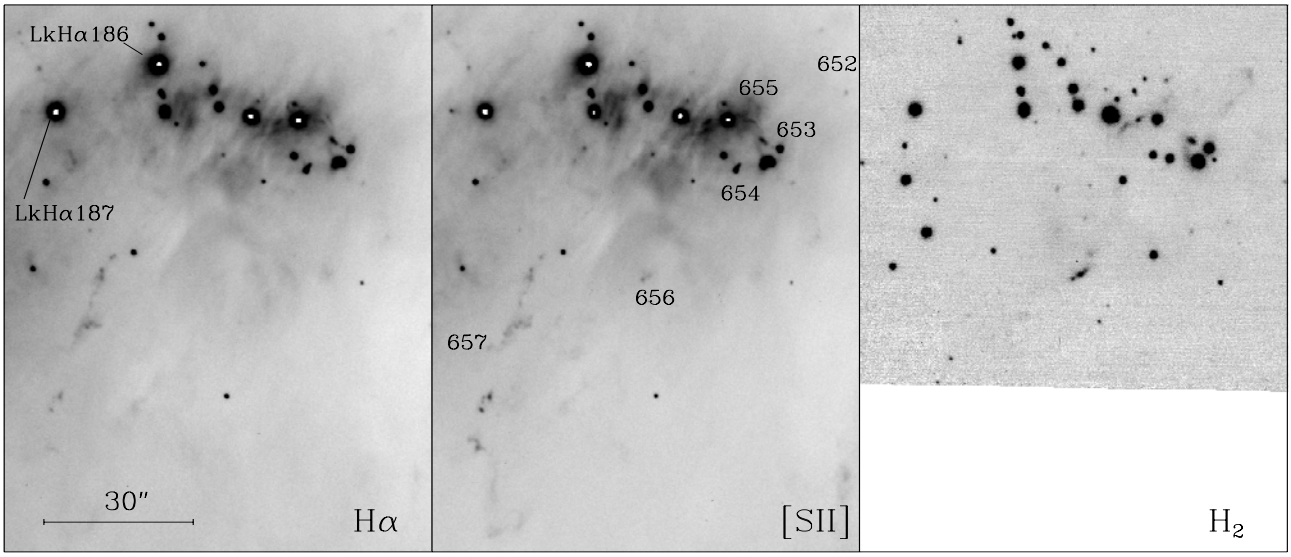

Fig. 6. The region of the optical cluster around LkHα 186 and the flows in Hα, [S II] and H_2 filters. We note that most of the flows are stronger in [S II], but there are some also strong in H_2, like HH 655 and 656, which are more embedded. To the northeast, an embedded flow in H_2 could be related to the optical knots of HH 652. In the H_2 image we also see the probable source of HH 654 just north of it, as well as other embedded point sources.

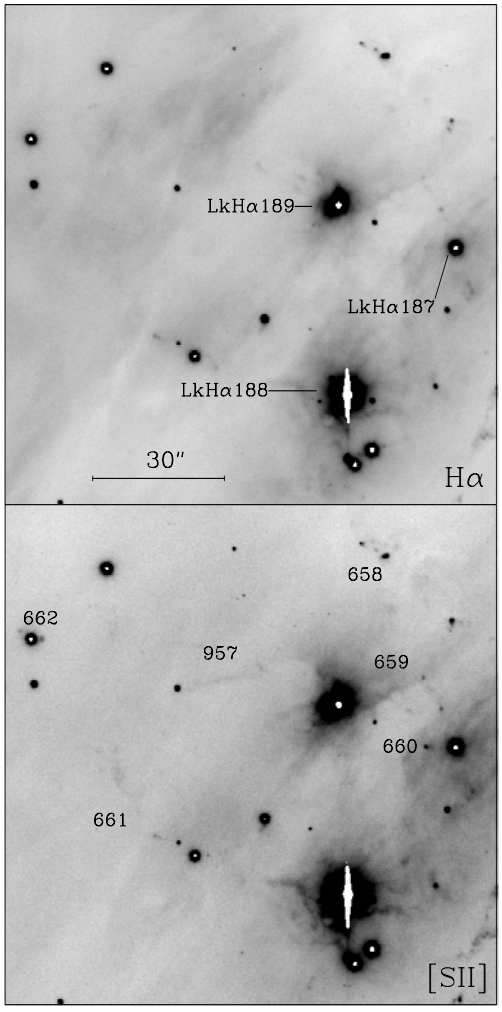

Fig. 7. East of the optical young cluster, LkHα 188 and 189 are surrounded by reflection nebulae. The HH objects found in the area are indicated in the [S II] image. HH 658 to 662 are mainly knots aligned pointing away from a star. The HH 957 weak jet was only distinguished with confidence in the recent Subaru images.

the wide field Subaru image are shown in Fig. 12, except HH 957, which is seen in Fig. 7. Table 3 lists the identifications, positions and a brief description of all the objects detected.

3.1. The region around the optical cluster of LkHα 186

In the region around the optical cluster the density of stars and shocks is so high that identification of the driving sources of flows is limited by confusion. Additionally, the stars of the cluster are surrounded by reflection nebulosity, especially the four brightest stars LkHα 186 to 189.

HH 652 (Fig. 6) is a single knot only seen in [S II]. In the H_2 image, there is a flow nearby but we cannot be sure if it is related to HH 652.

HH 653 seems to point away from the star MKHα 10 (MKHα is the designation for the new Hα emission-line stars; see next section). HH 653 is strong in all the three narrow band images and also shows a weak continuum component.

HH 654 is only detected in the optical narrow band images. It is very bright and points away from a source only seen in H_2 and JHK.

Star G4 (HBC 722) is surrounded by what we call HH 655, which consists of an eastern flow, stronger in [S II], but also very strong in H_2, plus a flow to the west and a knot to the north of the star. In the H_2 image there is also a diffuse nebulosity to the north, but west of the optical knot. With the present observations it is impossible to determine if all are in fact related to star G4.

HH 656 is stronger in [S II] than in Hα, and very strong in H_2. It lies at a position where it might be driven by a star faint in the optical, but bright in the near-infrared H_2 image, located 20″ to northwest.

HH 657 is a long flow with curved appearance which seems to point back at G1. But it is not entirely clear if the northern knots are really connected to the flows in the center. And also it is not clear if the southern part of the flow, resembling a bow shock, is related to HH 657 or to HH 656 or to none of them.

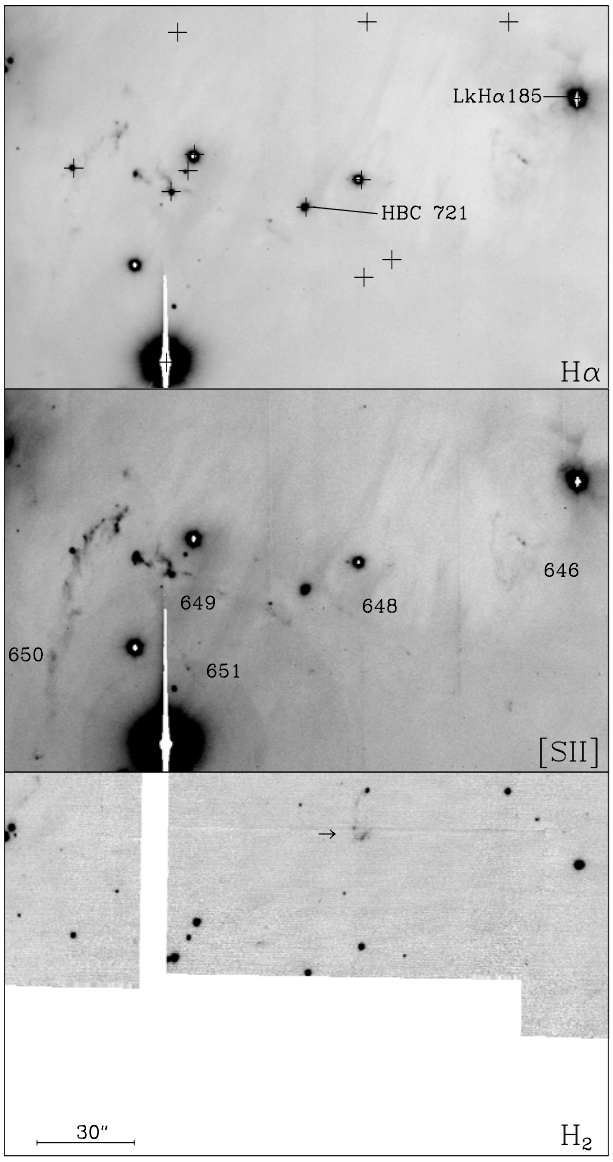

Fig. 8. Between the optical cluster and LkHα 185, the crosses in the Hα image mark the positions of the brightest sources in the 8 μm *Spitzer* images. In the [S II] image are marked the HH objects found. In the H_2 image an embedded flow is seen, only in the near infrared. Its probable source is barely seen in the optical images, but it is bright in the infrared images.

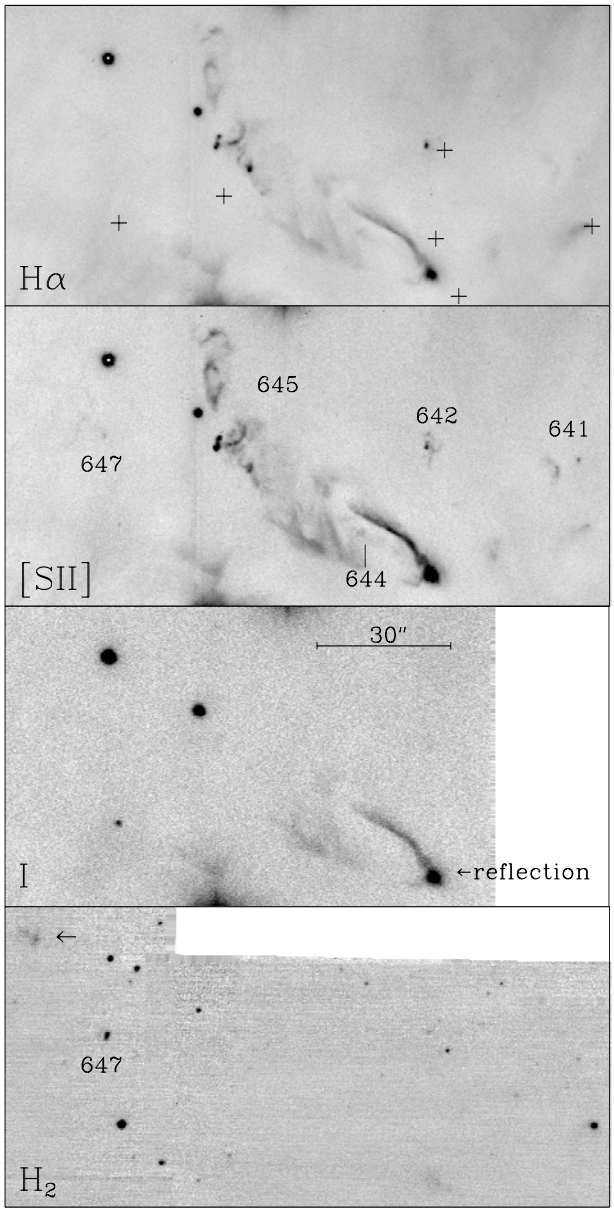

Fig. 9. The region around HH 644 and 645 in Hα, [S II], *I* and H_2. The bright point source and the curved filaments are actually reflection nebulae, visible at broadband *I*, and trace probably a cavity drawn by HH 644, which is only seen in [S II] and Hα. HH 647 is much brighter in the H_2 image, where there is also a nebulosity in the *upper left corner* of the image, not associated with optical structures. The strong *Spitzer* sources have their positions marked by a cross in the Hα image.

3.2. The region around LkHα 188–189

Figures 4 and 7 show the region east of the optical cluster, where LkHα 188 and LkHα 189 are very bright and immersed in diffuse emission.

HH 658 is a small chain of knots, strong in [S II] and Hα, pointing away from the direction of LkHα 186.

HH 659 and 660 are knots too, and both appear to come from LkHα 187, in different directions.

HH 661 has also two knots plus a fainter flow 25″ away. There is a possible counter-jet in Hα just southwest from the possible source, MKHα 24. Note that the fainter MKHα 26 also lies in a position where it could be the source of HH 661, or at least the nearest knots.

HH 662 consists of two single knots around MKHα 29, not perfectly aligned through the star.

The HH 957 weak jet was only distinguished with confidence in the recent Subaru images. It seems to point out of the faint star MKHα 27.

3.3. The region around HBC 721

West of the optical cluster (Figs. 4 and 8) the star HBC 721 is in the center of a chain of knots and filaments called HH 648, which seems to be a bipolar jet.

HH 646 is a faint structure and LkHα 185 could be its source.

HH 649 has a very strong knot, with a faint continuum component, a fainter filament pointing southwest, and another filamentary structure west of MKHα 8. It could be a bipolar jet from MKHα 8, although the filament is not perfectly aligned with it.

Table 3. Herbig-Haro objects in the Gulf of Mexico.

HH[a]	α(J2000)[b]	δ(J2000)[b]	[S II][c]	Hα[c]	H_2[c]	Comments[d]
636	20 57 45.5	43 52 47	y	y	n	2′ long
637	20 57 45.5	43 53 58	y	y	y	strong center, fainter structure 30″ N
638	20 57 51.6	43 51 40	y	y	–	strong knot plus filament
639	20 57 55.5	43 50 15	y	y	–	strong bow-shock plus larger fainter structure 1′ SE
640	20 57 47.3	43 53 25	y	y	y	extends to E and W, 1′ wide
641	20 57 52.7	43 54 02	y	w	n	bow plus knot 7″ NW
642	20 57 55.5	43 54 07	y	y	n	knot plus stucture ∼7″ wide
643	20 57 56.5	43 52 52	y	w	y	∼7″ wide
644	20 57 55.4	43 53 37	y	y	w	filament, extends 30″ to NE
645	20 57 59.6	43 54 07	y	y	n	extends to N and S, 40″ wide
646	20 58 01.4	43 53 07	y	y	n	knot plus bow, ∼25″ wide
647	20 58 02.3	43 54 09	w	n	n	weak, ∼20″ wide
648	20 58 01.8	43 52 17	y	w	n	3′ long chain of knots and filaments around HBC 721
649	20 58 12.5	43 53 03	y	y	n	strong knot plus filaments 1′ to SW
650	20 58 13.0	43 53 14	y	y	n	curved, extends 1.′5 to S
651	20 58 11.0	43 52 28	w	w	–	weak, 10″ long
652	20 58 14.9	43 53 49	w	n	w	weak knot
653	20 58 16.4	43 53 40	y	y	n	strong, points away from MKHα 10
654	20 58 16.9	43 53 33	y	y	n	strong, stellar-like
655	20 58 17.1	43 53 47	y	w	y	around star G4, 18″ wide
656	20 58 18.6	43 53 11	y	w	y	weak, extends 35″ to SE
657	20 58 21.5	43 52 47	y	w	n	1.′3 long
658	20 58 21.7	43 54 14	y	y	n	chain of knots 36″ to NE
659	20 58 21.9	43 53 54	y	y	n	knots, extends 30″ to NE
660	20 58 22.2	43 53 45	y	w	n	knot plus faint stucture 10″ to NE
661	20 58 27.9	43 53 25	y	w	–	knot plus larger sturcture 25″ to NE
662	20 58 30.3	43 54 09	y	n	–	two knots, W and NE of star MKHα 29
663	20 58 29.0	43 51 35	w	n	–	faint
952	20 56 23.2	43 43 55	w	n	–	three weak knots across nebulous star
953	20 56 41.6	43 48 39	y	y	–	very strong 24″ wide
954	20 56 57.6	43 40 38	w	n	–	1.′2 SW from nebulous star
955	20 58 14.3	43 46 13	y	n	–	triangular shape, 1.′5 SE from nebulous star
956	20 57 02.8	43 41 46	y	n	–	knot near nebulous star
957	20 58 26.5	43 54 00	w	n	–	weak jet-like 25″ long, W from star MKHα 28
958	20 58 28.3	43 56 44	w	n	–	chain of four knots 1′ long
p	20 56 21.0	43 47 33	w	w	–	weak knots
p	20 57 21.0	43 49 28	w	w	–	weak knots
p	20 58 06.4	43 53 01	w	w	n	knot near MKHα 6
p	20 58 08.0	43 40 27	w	?	–	10″ long structure, confusion with reflection area
p	20 58 24.1	43 50 43	w	n	–	weak, similar to HH 663

Notes. [a] HH 636 to 663 from 2002 observations, HH 952 to 958 from 2006 observations, p means possible HH objects that need confirmation. [b] The positions are measured at the brightest point. [c] Indicates if the flow is observed at each filter. y means yes, n means no, w means weak and - means it is out of the observed field in that filter. [d] Approximate description of how the HH object appears in the [S II] image.

Our near-infrared *JHK* images show a fainter redder star east of MKHα 8 and the filament next to HH 649's head points directly to it. We also see two embedded sources to the west in the *Spitzer* images, which lie in the direction of this flow. The positions of the bright *Spitzer* sources are marked with a cross in the figures.

HH 650 resembles HH 657 in structure, shape and orientation. It is a curved flow, more than 1.′5 long. A faint near-infrared source is located at the northern tip of the flow. There is also a bright infrared source (corresponding to IRS 6 from Cohen & Kuhi 1979) ∼25″ south of the flow.

HH 651 is a faint knot seen both in [S II] and Hα and a fainter filament only seen in [S II]. There is no indication of its source.

3.4. A reflection cavity

To the west (Fig. 9), the curved bright filament around HH 644 is due to reflected light, probably the wall of a cavity formed by a molecular outflow and illuminated by the embedded driving source. Faint reflected light can also be seen from the opposing wall. HH 644 is a knot plus a filament seen in Hα, stronger in [S II]. No probable source is seen in our optical or near-infrared images. In the *Spitzer* images we can see many embedded sources in the area, one coincides with the expected position of a source for HH 644 just southwest of the cavity.

HH 645 is possibly an extension of HH 644, but we cannot be sure of this without proper motion measurements. There are two *Spitzer* sources, one just northeast of the probable source of HH 644, and another source about 30″ northeast which also could be related to HH 645. There are two faint emission patches stronger in Hα west of the reflection nebula which are probably HH objects associated with a near infrared source seen in the H_2 image and also by *Spitzer*. We need confirmation of their nature, however, because they are stronger in the Hα images and they lie in a region where we lack corresponding broadband *I* images, so they could in principle be parts of an illuminated cavity, and are therefore not given HH numbers here.

HH 641 and HH 642 are diffuse structures, and there is one *Spitzer* source almost coinciding with HH 642.

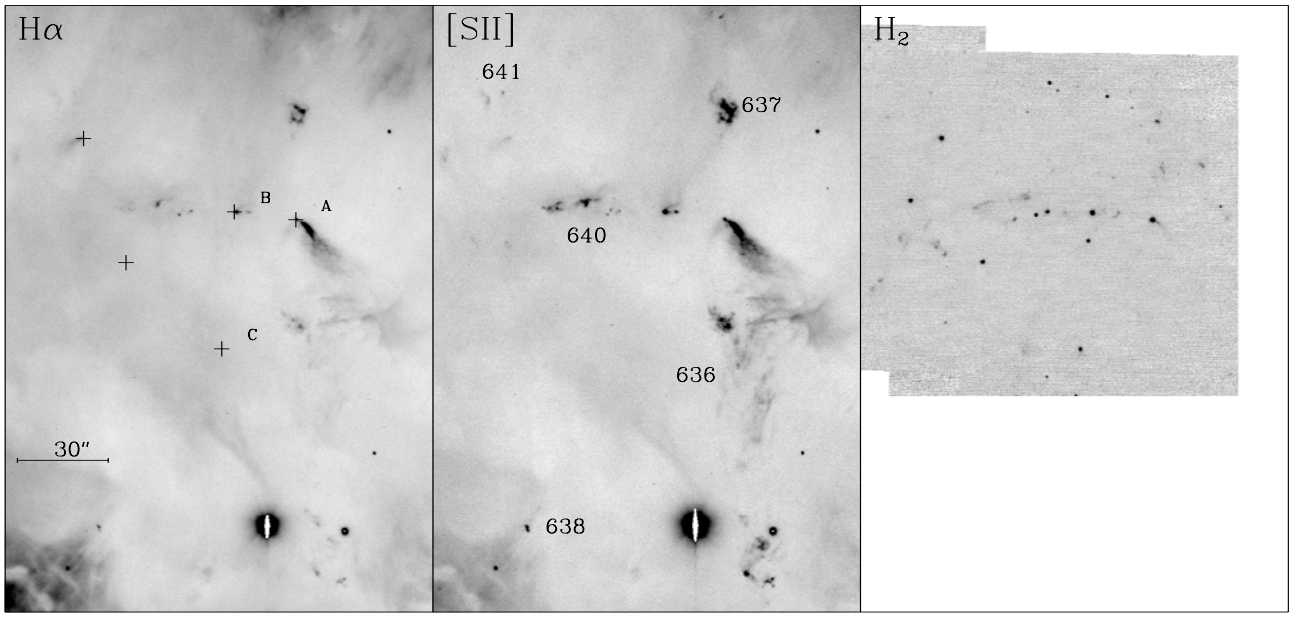

Fig. 10. The western-most flows in Hα, [S II] and H_2. In the H_2 image embedded flows and sources are seen. The strong *Spitzer* sources have their positions marked by a cross. Star marked A is a possible source for HH 636 and HH 637, B is likely the source of HH 640 and C is possibly related to HH 638.

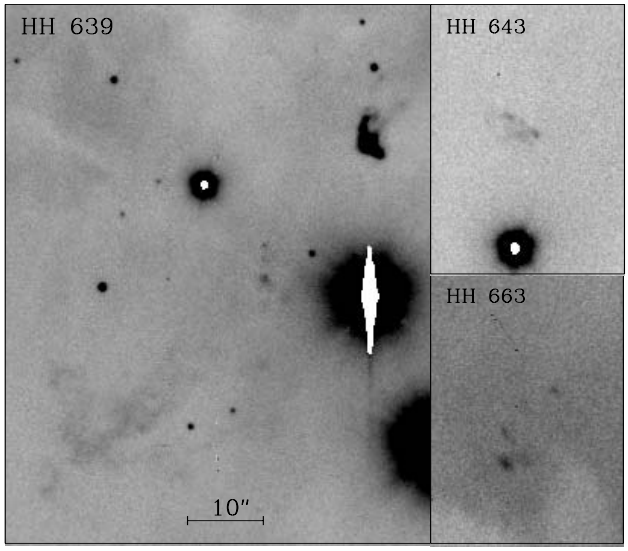

Fig. 11. HH 639, HH 643 and HH 663 in [S II] images at same scale.

HH 647 is very faint in the optical, but strong in the H_2 image. To its south there is one point source, faint in the optical, stronger in near-infrared and even brighter in *Spitzer* images, and it could be associated with this HH object. There are other probable flows in H_2 in this region, as seen in Figs. 8 and 9.

3.5. The westernmost flows

The western flows HH 636, 637, 638 and 640 are shown in Fig. 10. They are very bright in [S II] and not so faint in Hα. There is also an extended reflection nebula, bright in the broad band *R* images, probably an illuminated cavity. Unfortunately our *I*-band image does not cover this region.

Based on the geometry of the flows and the near-infrared appearance of the point sources, HH 636 and 637 appear to be part of a bipolar flow driven by the western star, visible in the H_2 image and also bright in *Spitzer* images, marked A in Fig. 10.

The star to the east (B), also bright in *Spitzer* images and showing signs of a cavity, is probably the source of HH 640, which shows a small flow to the west and a larger flow to the east of the star. The H_2 images show components of HH 640 and HH 637.

HH 638 is a bright knot and a faint filament that point back to a red source seen in our near-infrared images and also in the *Spitzer* images, marked C in the figure.

In Fig. 11, HH 639 is a very bright bow and a fainter larger bow to the southeast. HH 643 is faint even in [S II], visible in H_2. HH 663 is faint and visible only in the [S II] image. There are no conclusive candidate sources for these HH objects.

3.6. The newest flows

Figure 12 shows 6 of the 7 HH objects identified in the new wide-field Subaru images, most of them in the southwestern region of the Gulf of Mexico, far from the region where the major activity was detected first.

HH 952 is a chain of three faint knots whose axis passes through a nebulous star, with an illuminated cavity.

HH 953 is a bright object, with no candidate source identified.

HH 954 and HH 956 are faint objects found near a nebulous star.

HH 955 is faint and located near a reflection nebula that resembles a nearly edge-on disk. There is a source associated with this reflection in the optical and infrared, but its 2MASS colors show no infrared excess.

HH 958 is located north of the optical cluster, it is probably related to nearby infrared sources seen by *Spitzer*.

Other possible HH objects were found and are listed as "p" in Table 3, but further observations are needed to confirm their true nature, because they are too weak and/or lack corresponding broadband images.

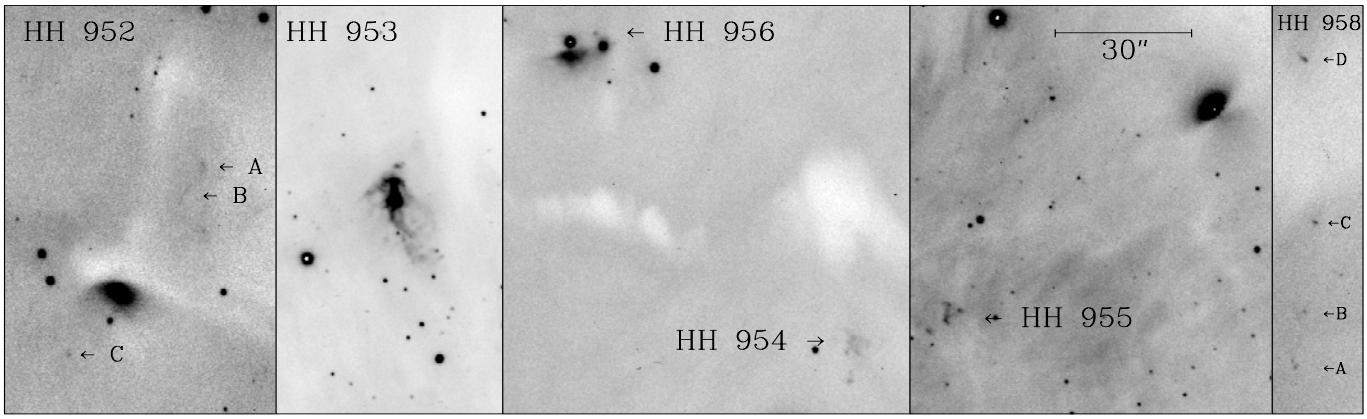

Fig. 12. The new HH objects found in the large-field Subaru [S II] images. All the images are at the same scale. HH 957 is displayed in Fig. 7.

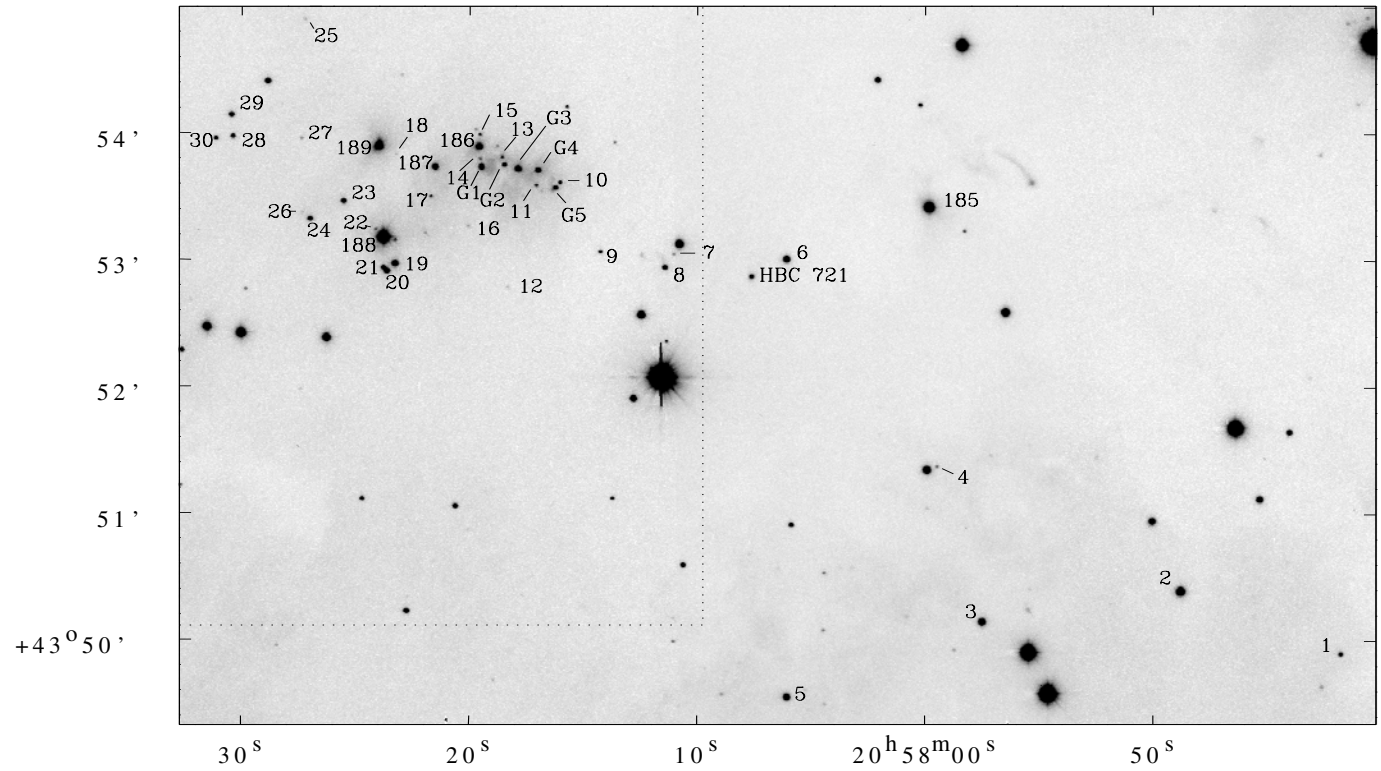

Fig. 13. *R* band image showing the Hα emission-line stars found. The numbers between 1 and 30 are the MKHα identification from the present work (Table 4). Stars with previous identifications did not receive new numbers. Labels between 185 and 189 refer to LkHα numbers. The dotted lines mark the smaller field area of the grism images taken in 1998.

4. New Hα emission-line stars

In our grism images using the Hα filter, the emission line is approximately centered in the slitless spectra and it is rather easy to detect the point-like emission. The images are deep and we can detect the continuum of stars down to approximately $R = 21$ mag.

A total of 41 Hα emission-line stars were found in the region surveyed (see Fig. 13 and Table 4), which corresponds to approximately 50% of the stars visible in our grism images. They are located mostly around the LkHα 186 cluster, but there are also Hα emission-line stars to the west. 90% of the stars within 2′ from LkHα 189 show emission in Hα.

Some of the stars were known from Herbig (1958), Cohen & Kuhi (1979) and Kohoutek & Wehmeyer (1999), listed in Table 1. The previously unknown emission-line stars are identified by us with MKHα numbers (MK stands for Mauna Kea).

Among the stars from Kohoutek & Wehmeyer (1999) corresponding to the IRS stars from Cohen & Kuhi (1979), IRS 3 (KW 53-11) is identified in both catalogs as a star around magnitude 17. We do not see emission from this star, but detected Hα emission in a fainter star, which we called MKHα 4, with magnitude 22, just northeast from the brighter star. IRS 4 is outside of our grism field and IRS 6 was – at the time of our observations – optically too faint to be detected. We could only find a correspondence to IRS 5, the optically visible HBC 721. The other optically visible stars with an Hα emission line listed in Table 1 were all detected in our survey.

The photometric survey from Laugalys et al. (2006) covers the entire region of the Gulf of Mexico with a limiting magnitude of $V = 17.5$ mag. They suspect the presence of Hα emission

Table 4. Hα emission-line stars in the Gulf of Mexico.

MKHα	Alt. Name[a]	α(2000)	δ(2000)	V	R	I	J^b	H^b	$K_s{}^b$	$W_{(2002)}{}^c$	$W_{(1998)}{}^c$
1		20 57 41.8	+43 49 54	20.85	19.37	–	13.97	13.16	12.86	9	
2	L III-1	20 57 48.9	+43 50 24	17.17	16.18	–	12.56	11.96	11.73	12	
3	L II-114	20 57 57.5	+43 50 10	17.82	16.85	16.28	13.84	13.14	12.91	7	
4		20 57 59.5	+43 51 23	22.17	20.75	18.94	15.70	14.78	14.34	8	
	LkHα 185	20 57 59.9	+43 53 26	16.22	15.08	14.60	11.85	10.87	10.25 $^+$	219	
5	L II-122	20 58 06.1	+43 49 34	18.32	17.28	16.39	13.89	13.12	12.78	46	
6		20 58 06.2	+43 53 01	17.93	16.74	15.95	13.41	12.58	12.21	29	
	HBC 721	20 58 07.6	+43 52 53	20.55	18.90	17.52	14.10	12.79	11.98 $^+$	50	
7		20 58 11.1	+43 53 04	22.86	20.97	18.66	14.79	13.86	13.38	13	–
8		20 58 11.4	+43 52 58	16.63	16.43	16.14	13.75	12.21	11.21 $^+$	104	97
9		20 58 14.3	+43 53 05	20.89	19.44	17.53	14.17	13.39	12.94	35	45
10		20 58 16.1	+43 53 37	21.22	19.38	17.43	13.46	11.33L	10.58L	25	26
	G5	20 58 16.3	+43 53 35	20.24	18.53	16.94	13.03	11.21L	10.42L	17	22
	G4	20 58 17.0	+43 53 43	19.09	17.67	16.55	13.25	12.21	11.46 $^+$	69	68
11		20 58 17.1	+43 53 36	21.77	20.15	18.00	14.09L	13.00L	12.96	13	22
	G3 *	20 58 17.9	+43 53 44	18.58	16.84	15.48	11.77	10.42	9.70	29	11
12		20 58 18.4	+43 52 48	23.47	22.02	19.53	15.63	14.91	14.32 $^+$	4	–
	G2	20 58 18.5	+43 53 47	20.53	18.75	17.08	13.21L	12.18	11.39	26	30
13		20 58 18.6	+43 53 49	21.83	19.90	18.30	13.39L	12.76	11.96	5	9
	G1 *	20 58 19.5	+43 53 45	19.34	17.65	16.18	12.62	11.35	10.84	7	–
14	*	20 58 19.6	+43 53 48	22.71	20.58	18.90	–	–	–	5	15
15		20 58 19.6	+43 54 00	21.70	20.13	18.08	13.79L	13.69	13.29	4	–
	LkHα 186	20 58 19.6	+43 53 55	18.12	16.68	15.85	12.69	11.49	10.92	30	33
16		20 58 20.1	+43 53 17	23.30	21.60	19.49	15.93	14.85	14.48	7	–
	LkHα 187	20 58 21.6	+43 53 45	18.56	17.05	16.00	12.80	11.49	10.71 $^+$	162	40
17		20 58 21.7	+43 53 31	22.40	20.62	18.17	13.77	12.36	11.80	9	–
18		20 58 23.3	+43 53 51	–	22.27	18.10	15.82	14.88	14.41	6	nc
19		20 58 23.3	+43 52 59	17.81	16.62	15.65	12.77	11.81	11.34	40	25
20		20 58 23.7	+43 52 56	18.30	16.98	15.87	12.87	12.07	11.74	24	12
21		20 58 23.9	+43 52 57	18.62	17.29	16.06	–	–	–	10	4
	LkHα 188	20 58 23.8	+43 53 12	14.65	13.69	13.37	10.56	9.62	8.84 $^+$	98	28
	LkHα 189	20 58 24.0	+43 53 55	17.10	15.80	15.03	12.23	11.16	10.69	92	29
22		20 58 24.4	+43 53 15	20.79	19.56	18.31	–	–	–	15	–
23		20 58 25.6	+43 53 29	19.58	18.11	16.81	13.60	12.40	11.73	46	37
24		20 58 27.1	+43 53 20	19.54	18.20	17.26	14.02	12.92	12.25 $^+$	144	45
25		20 58 27.3	+43 54 55	23.65	21.81	19.98	15.87	15.03	14.40 $^+$	6	nc
26		20 58 27.4	+43 53 24	23.60	21.78	19.86	16.08	15.03	14.34 $^+$	5	–
27		20 58 27.5	+43 53 58	22.80	21.51	19.41	15.28	14.32	13.79	3	15
28		20 58 30.4	+43 53 59	19.87	18.61	17.41	14.82	13.67	12.89 $^+$	70	42
29		20 58 30.5	+43 54 10	20.68	19.20	17.63	13.79	12.84	12.41	69	17
30		20 58 31.2	+43 53 58	19.10	17.78	16.63	15.33	14.04	13.29	4	5

Notes. [(a)] LkHα numbers from Herbig (1958); G numbers from Cohen & Kuhi (1979); HBC number from Herbig & Bell (1988); L numbers from Laugalys et al. (2006), with possible Hα emission. [(b)] JHK_s magnitudes extracted from the 2MASS All-Sky Catalog. All magnitudes marked L are upper limits. [(c)] Hα equivalent widths measured in 2002 and 1998 images. *nc* means Hα emission with no or very faint continuum. * Visual binaries. $^+$ Stars with infrared excess in the JKH color–color diagram (Fig. 15).

in nine stars in the region surveyed by us, including LkHα 185, 188, 189, MKHα 2, 3 and 5, in all of which we detect Hα emission. The other three stars were also checked on our grism images and no emission lines were seen (stars II-109, 113 and 118 in their Table 2). Their limiting magnitude prevented them from detecting other known emitters in the area, such as LkHα 186 and 187. In their recent spectroscopic follow-up, Corbally et al. (2009) confirm the Hα emission lines also seen by us in MKHα 2, 3 and 5 and determine their spectral types (M3.5e, M1e and K7e, respectively). They put MKHα 2 at a distance of 137 pc from the Sun, excluding it from the star formation complex. MKHα 3 and 5 might have distances compatible with the complex. They classify II-109 and II-113 as G-type stars with Hα filled in with emission, which explains why we did not detect the emission in our grism images.

In first-epoch grism images obtained in 1998 by George Herbig and kindly put at our disposal, almost all the Hα emission-line stars were also detected (25 out of the 33, in the common field of view). The equivalent widths of the lines were measured at both epochs and in almost all of the cases the Hα emission line strength is comparable (see Table 4).

In the recent Subaru images obtained in very good seeing it is possible to resolve three of the stars in the cluster as doubles, with angular separations of less than 1″: G1, G3 and MKHα 14. Because of the limited resolution in the grism images, it is not possible to confirm if both components in each system have emission, but we see tentative evidence that this is true at least in the case of MKHα 14.

Table 4 lists the 41 Hα emission-line stars identified. The first column gives an MKHα (Mauna Kea) identification number to all the stars previously unknown as Hα emitters. Column two gives the identification for the previously known emission-line stars, as well as other possible designations. Columns three and four give coordinates of the stars. The following three

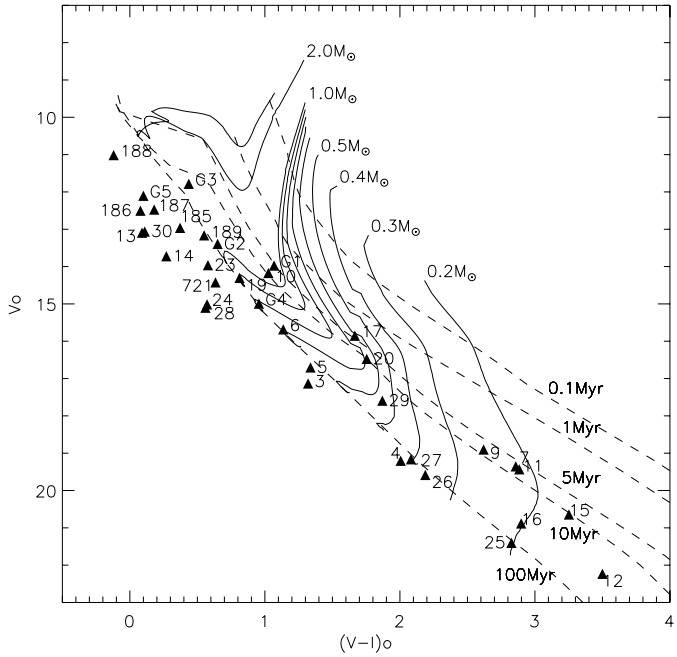

Fig. 14. Color–magnitude diagram for the Hα emission-line stars (triangles). An extinction-correction was applied to obtain V_0 and $(V-I)_0$ values. The solid lines are evolutionary tracks from D'Antona & Mazzitelli (1997), for masses from 0.2 to 2.0 $M_\odot$ and the dashed lines are their 0.1, 1, 5, 10 and 100 Myr isochrones. The stars are labeled as in Fig. 13.

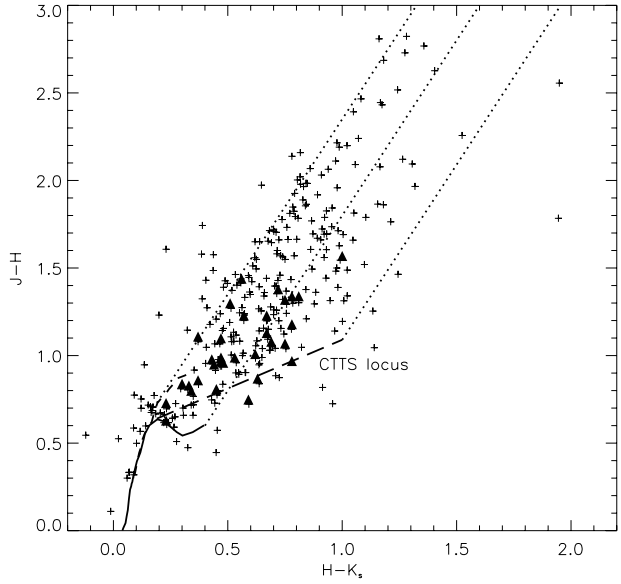

Fig. 15. JHK_s diagram of the stars detected in all the 3 bands with 2MASS in the region surveyed. Solid triangles are the Hα emission-line stars in Table 4. The solid and dashed lines are, respectively, the location of main sequence and giant stars from Bessell & Brett (1988) corrected to the 2MASS photometric system (Carpenter 2001). The long-dashed line represents the CTTS location from Meyer et al. (1997). The dotted lines show the direction of the interstellar reddening vectors from Straižys et al. (2008).

columns provide the optical *VRI* magnitudes obtained in our observations, while the next three columns list the near-infrared JHK_s magnitudes obtained from the 2MASS All Sky Survey Catalog. The Hα emission line equivalent widths measured in 1998 and 2002 are provided in the last two columns of the table. The optical binaries are also marked in the table, as well as the stars showing near-infrared excess (see next section).

From the previously known spectral types of nine of the stars we have determined expected main-sequence $(J-H)_0$ colors from Bessell & Brett (1988) and estimated extinction values (A_V) for those stars. The same information was also obtained by de-reddening the stars down to a location on the main sequence in the $(J-H)\times(H-K_s)$ diagram shown in the next section. The method is described in Herbig & Dahm (2006). The values obtained using both methods agree within 0.6 mag. The method of de-reddening was applied to all the stars that have *JHK* colors.

The extinction-corrected V_0 magnitudes and $(V-I)_0$ colors enabled us to place the stars in a color–magnitude diagram, from which we can get a rough estimate of their masses and ages. That diagram is shown in Fig. 14. The evolutionary tracks and isochrones from D'Antona & Mazzitelli (1997) were translated into the observational plane using the relationships of Hillenbrand (1997). Most stars seem to have masses between 0.2 and 1 $M_\odot$, with LkHα 188 showing highest mass and MKHα 12 the lowest. All the optically visible Hα emission stars are older than 5 Myr. Note that the errors in the A_V values can lead to errors of about 30% in the estimate of their masses.

5. Embedded sources

We use the JHK_s 2MASS magnitudes of the stars in the field surveyed to make a color-color diagram (Fig. 15) to identify stars with infrared excess, indicating the presence of a disk. The figure shows the location of main sequence and giant stars from Bessell & Brett (1988) in solid and short-dashed lines respectively. The Classical T-Tauri Stars (CTTS) location from Meyer et al. (1997) is also indicated as a long-dashed line. A correction to the 2MASS photometric system was performed following the prescription of Carpenter (2001). The three parallel dotted lines show the direction of the interstellar reddening vectors determined for the L935 region by Straižys et al. (2008). All the stars falling to the right of the middle vector have clear infrared excess, they constitute about 25% of the stars in the figure.

The Hα emission-line stars are marked as triangles in the JHK_s diagram and 11 of them show some infrared excess. Those stars are marked in Table 4. So, 70% of the Hα emission-line stars show colors typical of more evolved young stars with limited circumstellar material. LkHα 188 is the emission-line star with larger infrared excess, but apparently only little extinction.

8 out of the 10 stars with Hα emission line equivalent width larger than 50 Å have infrared excess. The other 3 stars with infrared excess have a very small Hα emission line equivalent width ($\leq$6 Å).

The *JHKL* IRTF images cover only the central cluster area, so we extracted near-infrared photometry only for those stars that fall inside the IRTF 75″ field of view. The magnitudes obtained are listed in Table 5, as well as the coordinates, a near-infrared identification number (NIR Id.) and its correspondence to a MKHα number when one exists. Figure 16 shows all the four IRTF images, with the identification numbers for the near-infrared stars detected, as in Table 5, and also the corresponding *Spitzer* images at 8 μm and 24 μm.

A color–color diagram was plotted in a similar way to the one built with 2MASS magnitudes (Fig. 17). This time the locations of main sequence and giant stars were not corrected for the 2MASS photometric system, as we use the standard IRTF *JHK* filters. Among the 23 stars detected in all the three bands, 9 have

Table 5. *JHKL* observations of the LkHα 186 cluster.

NIR Id	Hα Id	α(2000)	δ(2000)	J	H	K	L
1		20 58 15.7	+43 54 12	16.39	15.62	15.65	–
2		20 58 15.8	+43 53 12	16.15	15.33	14.72 $^+$	–
3		20 58 16.0	+43 53 35	16.07	14.83	14.10 $^+$	–
4	MKHα 10	20 58 16.1	+43 53 37	13.49	12.04	11.38	8.21
5	G5	20 58 16.3	+43 53 35	13.36	11.70	10.79 $^+$	7.30
6		20 58 16.4	+43 53 22	–	–	15.70	–
7		20 58 16.8	+43 53 36	17.49	14.22	12.27 $^+$	8.44
8	G4	20 58 17.0	+43 53 43	13.18	12.00	11.41	7.69
9		20 58 17.1	+43 53 17	17.17	14.42	12.72 $^+$	9.06
10	MKHα 11	20 58 17.1	+43 53 36	14.24	13.30	12.94	–
11		20 58 17.7	+43 53 31	15.37	13.77	12.89 $^+$	9.61
12		20 58 17.8	+43 53 47	15.85	14.39	14.07	–
13	G3	20 58 17.9	+43 53 44	11.72	10.33	9.65	6.24
14		20 58 18.4	+43 53 24	–	–	15.68	8.89
15	G2	20 58 18.5	+43 53 47	13.62	12.13	11.46	8.20
16	MKHα 13	20 58 18.6	+43 53 49	14.38	12.74	11.97	8.95
17		20 58 18.8	+43 53 54	14.29	13.19	12.69	9.75
18	G1	20 58 19.5	+43 53 45	12.66	11.32	10.82	7.86
19	MKHα 14	20 58 19.6	+43 53 48	15.27	13.56	12.54 $^+$	9.16
20	MKHα 15	20 58 19.6	+43 54 00	14.55	13.76	13.49	–
21	LkHα 186	20 58 19.6	+43 53 55	12.63	11.39	10.84	7.52
22		20 58 19.8	+43 54 02	15.34	14.19	13.63	–
23	MKHα 16	20 58 20.1	+43 53 17	15.68	14.74	14.25	–
24		20 58 21.2	+43 53 27	18.09	16.35	15.20 $^+$	–
25		20 58 21.3	+43 53 21	15.69	13.05	11.60 $^+$	8.50

Notes. $^+$ Stars with infrared excess according to the *JHK* color–color diagram (Fig. 17).

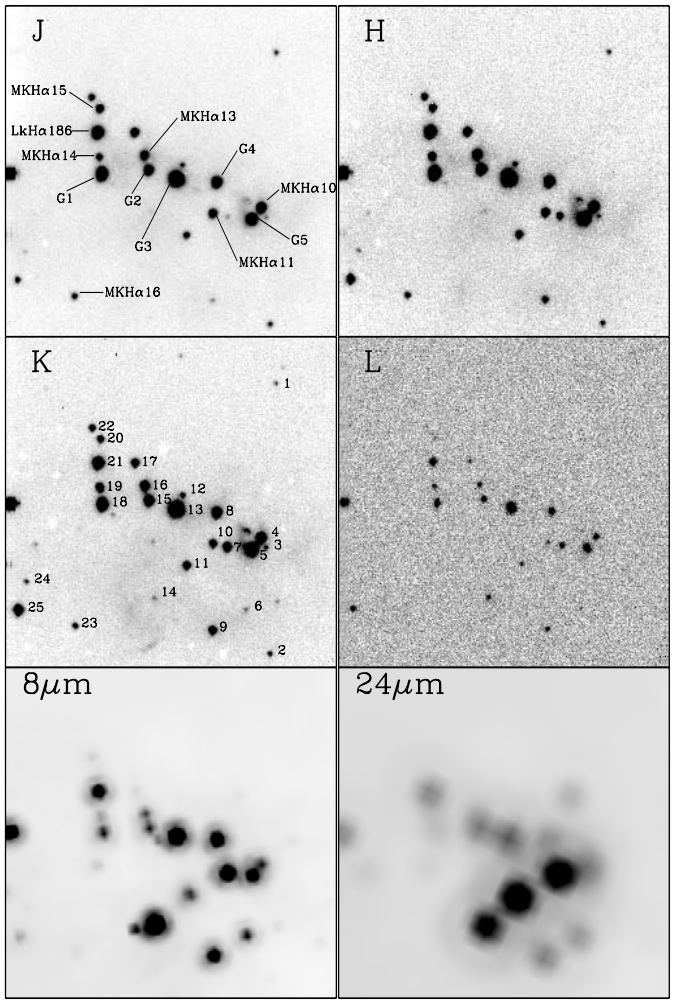

Fig. 16. *J*, *H*, *K* and *L* images, with the NIR identification numbers for the LkHα 186 cluster used in Table 5 shown in the *K* image and previous designations shown in the *J* image. At *the bottom*, the corresponding area as observed by *Spitzer* at 8 μm and 24 μm. Each image is 75″ on the side.

infrared excess (39%). Our observations are concentrated in a small area where it is likely that almost all the stars are part of the young population. The relatively high fraction of stars with little or no excess emission suggests that the overall population is already several million years old.

Spitzer magnitudes extracted for IRAC 3.6, 4.5, 5.8 and 8.0 μm and MIPS 24 μm are listed in Table 6, for both the Hα emission-line stars and the NIR stars detected in the IRTF images. A color–color diagram (Fig. 18) was built in order to classify the stars according to the regions they occupy in the diagram (Allen et al. 2004). The majority of stars lie in the region of Class II (Classical T-Tauri) stars. Most of the Class I stars are possible sources of HH objects. Stars that fall in the Class III (Weak-line T-Tauri) region indeed show weak or no Hα emission-line.

Near the optical cluster, the most embedded sources lie to its south, as shown in the *Spitzer* 8 μm and 24 μm images (Fig. 16). At 24 μm NIR 7, 11 and 14 become significantly brighter than the others. Star NIR 7 is located in the upper right corner of the *JHK* color–color diagram, it is one of the stars with higher infrared excess and it is heavily extincted. It is barely seen at *J* and becomes brighter as we move to longer wavelengths. It is located near HH 654 and is likely its source. In the *Spitzer* color-color diagram, it could be a Class II star, given the amount of extinction it has. Star NIR 11 shows relatively large extinction, but no significant infrared excess in *JHK*. Star NIR 14 is only seen at *K* and *L* and is close to a nebulosity seen at *K* and an H_2 flow associated with HH 656. Its position indicates that it could be the source of this flow. Both NIR 11 and NIR 14 are classified as Class I protostars, as well as NIR 6, NIR 9, MKHα 8 and HBC 721. MKHα 8 is the emission-line star with larger extinction in the JHK_s diagram (Fig. 13). In the *JHK* diagram of Fig. 17, NIR 9 and NIR 25 also show a large amount of extinction, both lie to the south of the optical cluster. NIR 25 is located in the Class III region of the *Spitzer* color–color diagram.

6. Conclusions

We have surveyed the region of the Gulf of Mexico around the little optical cluster that contains LkHα 185 to 189 using Hα and [S II] filters and we found 35 new HH objects. The average projected extent of the larger flows is approximately 1′, which, at a distance of 550 pc, corresponds to ~0.15 pc.

Without proper motions it is rather difficult to identify the source of each of the new flows. Images taken over several years may reveal the overall motion of the HH objects, aiding in the identification of their sources. Our images span only from 2002 to 2006 and reveal no sign of proper motion. Based on our best resolution of 0.20″/pix, we estimate that the tangential velocities cannot be larger than 120 km s^{-1}, giving the assumed distance. This is similar to the typical velocities seen for HH flows.

A search for Hα emission-line stars resulted in the detection of many more young stars than previously known; 41 in the 14′× 7′ region surveyed, of which 30 are new. Also, near-infrared images confirm that there are many embedded young sources and flows in the region. Classification based on *Spitzer* IRAC colors is provided for most of the sources. Almost all the Hα emission-line stars are Class II stars. Class I protostars are found mainly among the near-infrared sources and are located south and west

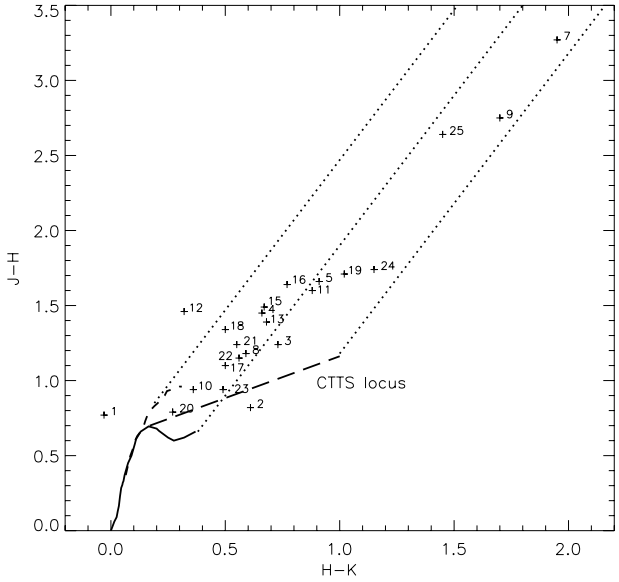

Fig. 17. *JHK* diagram of the LkHα 186 cluster showing the stars detected in the IRTF *J*, *H* and *K* images. The solid and dashed lines are, respectively, the location of main sequence and giant stars from Bessell & Brett (1988) and the long-dashed line represents the CTTS location from Meyer et al. (1997). The dotted lines show the direction of the interstellar reddening vectors from Straižys et al. (2008). The stars with infrared excess are marked in Table 5.

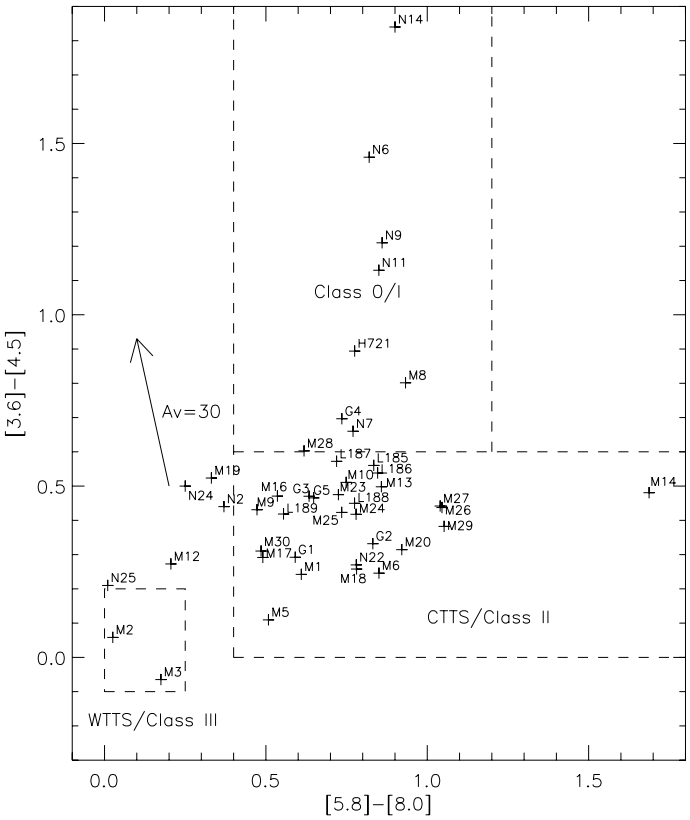

Fig. 18. An SPITZER/IRAC color–color diagram showing the positions of the Hα emission-line stars as well as the NIR stars. M stands for MKHα emission-line stars, N stands for NIR stars, H stand for HBC and G is the Cohen & Kuhi (1979) designation for emitters in the LkHα 188 cluster.

Table 6. IRAC and MIPS magnitudes for the Hα emission-line stars and the embedded NIR stars.

Id	[3.6]	[4.5]	[5.8]	[8.0]	[24]	Class.[a]
MKHα 1	12.40	12.16	11.78	11.17	7.96	II
MKHα 2	11.47	11.41	11.33	11.30	–	III
MKHα 3	12.75	12.81	12.68	12.50	–	III
MKHα 4	14.05	13.93	13.88	–	9.55	III ?
LkHα 185	9.36	8.80	8.35	7.52	3.84	II
MKHα 5	12.61	12.50	12.41	11.90	7.35	II
MKHα 6	11.48	11.23	10.75	9.90	6.93	II
HBC 721	10.38	9.49	8.75	7.98	5.20	I
MKHα 7	12.39	11.88	–	–	–	II ?
MKHα 8	9.31	8.51	7.62	6.69	3.18	I
MKHα 9	12.12	11.69	11.32	10.85	–	II
MKHα 10	10.01	9.50	9.45	8.71	–	II
G5	9.11	8.65	8.64	7.99	–	II
G4	9.91	9.22	8.52	7.79	–	I/II
MKHα 11	11.92	11.29	–	–	–	II ?
G3	8.83	8.36	7.86	7.23	–	II
MKHα 12	13.80	13.53	13.41	13.20	–	III
G2	10.67	10.34	10.05	9.22	–	II
MKHα 13	11.00	10.50	10.07	9.21	–	II
G1	10.20	9.91	9.53	8.94	–	II
MKHα 14	11.43	10.94	10.61	8.93	–	II
MKHα 15	12.50	–	–	–	–	–
LkHα 186	9.98	9.44	8.96	8.11	4.87	II
MKHα 16	13.40	12.93	12.48	11.95	-	II
LkHα 187	9.41	8.84	8.31	7.59	5.03	II
MKHα 17	11.43	11.14	10.80	10.31	–	II
MKHα 18	13.24	12.98	12.51	11.73	–	II
MKHα 19	10.62	10.10	10.07	9.74	–	II
MKHα 20	11.19	10.87	10.43	9.51	–	II
MKHα 21	11.49	–	–	–	–	–
LkHα 188	7.88	7.43	7.05	6.27	3.60	II
LkHα 189	9.98	9.56	9.31	8.75	6.18	II
MKHα 22	–	–	–	–	–	–
MKHα 23	10.66	10.19	9.74	9.02	6.53	II
MKHα 24	11.21	10.79	10.55	9.77	7.27	II
MKHα 25	13.62	13.19	12.73	12.00	8.35	II
MKHα 26	13.39	12.95	12.44	11.39	–	II
MKHα 27	13.06	12.62	12.05	11.01	8.73	II
MKHα 28	11.71	11.10	10.54	9.93	7.34	II
MKHα 29	11.80	11.41	10.94	9.89	7.33	II
MKHα 30	12.05	11.74	11.49	11.00	7.62	II
NIR 1	15.27	14.97	14.48	–	–	II ?
NIR 2	13.85	13.41	13.25	12.88	–	II
NIR 3	–	–	–	–	–	–
NIR 6	12.02	10.56	9.70	8.88	4.61	I
NIR 7	9.96	9.30	8.62	7.85	3.40	I/II
NIR 9	10.79	9.58	8.88	8.02	4.51	I
NIR 11	11.71	10.58	9.67	8.82	3.27	I
NIR 12	–	–	–	–	–	–
NIR 14	10.85	9.01	7.79	6.89	3.39	I
NIR 17	11.37	–	–	–	–	–
NIR 22	12.55	12.28	9.74	8.96	4.87	II
NIR 24	11.89	11.39	10.58	10.33	–	II
NIR 25	10.76	10.55	10.36	10.35	–	III

Notes. [a] Classification according to color–color diagram in Fig. 18. ? indicates the classification is based only in the [3.6]–[4.5] color.

of the optical cluster. Our observations reveal that star formation is much more active in this area than previously suspected.

The exciting source of this entire HII region (2MASS J205551.25+435224.6), as identified by Comerón & Pasquali (2005), lies directly to the west of the region studied, less than 25′ away in projection, and presumably only slightly more

distant than the L935 cloud. Among the O-type candidates from Straižys & Laugalys (2008), 2MASS J205552.70+435324.2 lies very close to the Comerón & Pasquali (2005) source, and 2MASS J205806.73+435514.1 lies only 2′ northwest from the optical cluster of LkHα 188. It seems likely that the low-mass young stars we see represent second-generation star formation in the remnant clouds surrounding the W80 HII region which have been compressed by the central O-stars.

The optical cluster of the low mass Hα emission-line stars is only a small portion of the total number of stars being formed there, and is only one of eight clusterings in the region according to the recent *Spitzer* study by Guieu et al. (2009). The presence of numerous HH flows and many reddened sources indicates that this is a large site of widespread star formation, still partially embedded in the dark cloud. Further studies in the Gulf of Mexico are encouraged.

Acknowledgements. We are very grateful to George Herbig for placing his 1998 grism images and measurements at our disposal. T.A. is also thankful for many discussions and suggestions from Luiz Paulo R. Vaz. We thank the referee Fernando Comerón for suggestions that improved this paper. T.A. acknowledges financial support from CNPq/ Brazil under processes 200430/2001-7 and 201958/ 2007-4. B.R. was partially supported by the National Aeronautics and Space Administration through the NASA Astrobiology Institute under Cooperative Agreement No. NNA04CC08A issued through the Office of Space Science, and by the NSF through grants AST-0507784 and AST-0407005. This work made use of observations from the *Subaru Telescope*, which is operated by the National Astronomical Observatory of Japan, from the *Spitzer Space Telescope*, which is operated by the Jet Propulsion Laboratory, California Institute of Technology under a contract with NASA, from the *Infrared Telescope Facility*, which is operated by the University of Hawaii under Cooperative Agreement No. NCC 5-538 with the National Aeronautics and Space Administration, Science Mission Directorate, Planetary Astronomy Program, and from the *United Kingdom Infrared Telescope*, which is operated by the Joint Astronomy Centre on behalf of the Science and Technology Facilities Council of the UK We also acknowledge the use of data products from the *Two Micron All Sky Survey*, which is a joint project of the University of Massachusetts and the Infrared Processing and Analysis Center/California Institute of Technology, funded by NASA and NSF, and Digitized Sky Surveys (DSS) images, produced at the Space Telescope Science Institute under US Government grant NAG W-2166.

References

Allen, L. E., Calvet, N., DAlessio, P., et al. 2004, ApJS, 154, 363
Armandroff, T. E., & Herbst, W. 1981, AJ, 86, 1923
Bally, J., & Reipurth, B. 2003, AJ, 126, 893
Bally, J., & Scoville, N. Z. 1980, ApJ, 239, 121
Bessell, M. S., & Brett, J. M. 1988, PASP, 100, 1134
Carpenter, J. M. 2001, AJ, 121, 2851
Cohen, M., & Kuhi, L. 1979, ApJS, 41, 743
Comerón, F., & Pasquali, A. 2005, A&A, 430, 541
Corbally, C. J., Straižys, V., & Laugalys, V. 2009, Baltic Astron., 18, 111
D'Antona, F., & Mazzitelli, I. 1997, Mem. Soc. Astron. Ital., 68, 807
Guieu, S., Rebull, L. M., Stauffer, J. R., et al. 2009, ApJ, 697, 787
Herbig, G. H. 1958, ApJ, 128, 259
Herbig, G. H., & Bell, K. R. 1988, Lick Observatory Bull., 1111
Herbig, G. H., & Dahm, S. E. 2006, AJ, 131, 1530
Herbig, G. H., & Rao, N. K. 1972, ApJ, 174, 401
Hillenbrand, L. A. 1997, AJ, 113, 1733
Kohoutek, L., & Wehmeyer, R. 1999, A&AS, 134, 255
Laugalys, V., & Straižys, V. 2002, Baltic Astron., 11, 205
Laugalys, V., Straižys, V., Vrba, F. J., et al. 2006, Baltic Astron., 15, 483
Meyer, M. R., Calvet, N., & Hillenbrand, L. A. 1997, AJ, 114, 288
Miller, A. A., Hillenbrand, L. A., Covey, K. R., et al. 2011, ApJ, in press [arXiv:1011.2063v2]
Morgan, W. W., Strömgren, B., & Johnson, H. M. 1955, ApJ, 121, 611
Neckel, T., Harris, A. W., & Eiroa, C. 1980, A&A, 92, 9
Ogura, K., Sugitani, K., & Pickles, A. 2002, AJ, 123, 2597
Osterbrock, D. E. 1957, ApJ, 125, 622
Reipurth, B., & Schneider, N. 2008, in Handbook of Star Forming Regions, Vol. I, ed. Bo. Reipurth, ASP Monograph, 4, 36
Semkov, E., Peneva, S. P., Munari, U., Milani, A., & Valisa, P. 2010, A&A, 523, L3
Straižys, V., & Laugalys, V. 2008, Baltic Astron., 17, 143
Straižys, V., Kazlauskas, A., Vansevičius, V., & Černis, K. 1993, Baltic Astron., 2, 171
Straižys, V., Corbally, C. J., & Laugalys, V. 2008, Baltic Astron., 17, 125
Welin, G. 1973, A&AS, 9, 183
Wendker, H. J. 1968, Z. Astrophys., 68, 368
Wendker, H. J., Baars, J. W. M., & Benz, D. 1983, A&A 124, 116
Westerhout, G. 1958, Bull. Astron. Inst. Netherlands, 14, 215